Scientific Research

Synthesis of Bifunctional Poly(Vinyl Phosphonic Acid-*co*-glycidyl Metacrylate-*co*-divinyl Benzene) Cation-Exchange Resin and Its Indium Adsorption Properties from Indium Tin Oxide Solution

Chi Won Hwang, Chang Soo Lee, Taek Sung Hwang[*]
Department of Applied Chemistry and Biological Engineering, Chungnam National University,
Daejeon, Korea
Email: [*]tshwang@cnu.ac.kr

ABSTRACT

Poly(vinyl phosphonic acid-*co*-glycidyl methacrylate-*co*-divinyl benzene) (PVGD) and PVGD containing an iminodiacetic acid group (IPVGD), which has indium ion selectivity, were synthesized by suspension polymerization, and their indium adsorption properties were investigated. The synthesized PVGD and IPVGD resins were characterized using Fourier transform infrared (FT-IR) spectroscopy, scanning electron microscopy (SEM), energy-dispersive X-ray spectroscopy (EDS) and mercury porosimetry. The cation-exchange capacity, the water uptake and the indium adsorption properties were investigated. The cation-exchange capacities of PVGD and IPVGD were 1.2 - 4.5 meq/g and 2.5 - 6.4 meq/g, respectively. The water uptakes were decreased with increasing contents of divinyl benzene (DVB). The water uptake values were 25% - 40% and 20% - 35%, respectively. The optimum adsorption of indium from a pure indium solution and an artificial indium tin oxide (ITO) solution by the PVGD and IPVGD ion-exchange resins were 2.3 and 3.5 meq/g, respectively. The indium adsorption capacities of IPVGD were higher than those of PVGD. The indium ion adsorption selectivity in the artificial ITO solution by PVGD and IPVGD was excellent, and other ions were adsorbed only slightly.

1. Introduction

Rare metals with conductivity and transparency, such as indium, are essential for the production of display panels, such as LCD, OLED and PDP. China possesses most of the rare metals and recently weaponized these resources. Therefore, a secure supply of rare metals, which are necessary to the semiconductor industry and the munitions industry, is urgently needed. Intensive research on indium recovery technologies and material development have been conducted in developed countries (USA, Japan) to secure these resources from seawater and ITO etching waste fluid [1-4].

However, the amount of indium in seawater is very low. It is important to develop an adsorption and separation material with high selectivity. To separate indium from ITO waste fluid which is produced during the display etching process called "urban mining," the development of a selective adsorption and separation material for the recovery of indium from the etching waste fluid in highly acidic conditions is required [5-7].

Ion exchange resins are widely used for the recovery of indium from seawater due to the simplicity of the exchange process and the regeneration ability of the resin. However, the development of a highly selective ion exchanger is needed because the concentration of indium in seawater is low [8-12].

The chemical extraction method, which uses nitric acid or a combination of nitric acid and hydrochloric acid, the electro-dialysis method, and the ion exchange method are used for the recovery of indium from ITO etching

[*]Corresponding author.

fluid [2,4]. Chemical extraction using acids has high efficiency, but it is difficult to separate indium and tin because both of these elements are simultaneously extracted from seawater due to the difficulty involved in controlling the pH. The electrodialysis method has high selectivity, but it suffers from contamination of the membrane, which is a fundamental part of the electrodealysis method, due to the high acidity of the ITO etching waste fluid, which causes a decrease in selectivity. The ion exchange method can improve the weaknesses of other methods; however, it is necessary to develop a highly selective adsorption material for the recovery of traces of indium from dilute solutions.

The most widely used ion exchange resins have phosphate groups for the selective adsorption of indium. However, the development of a novel resin is necessary because these resins have low mechanical stability and low adsorption capability.

We synthesized a bifunctional poly(VPA-*co*-GMA-*co*-DVB) cation exchanger with a high ion exchange capacity, good mechanical strength, and easy functionalization capability of selective indium adsorption groups for the selective absorption and separation of indium. We investigated its structure, ion exchange capacity, water uptake, and the optimal conditions for the synthesis of the resin and the adsorption of indium via adsorption tests using artificial ITO solutions. In this paper, it was experimental with "February. 4. 2013. Chungnam National University, 79 Daehangno, Yuseong-gu, Daejeon 305-764, Republic of Korea".

2. Experimental

2.1. Materials

Vinyl phosphonic acid (VPA, 90%), glycidyl metacrylate (GMA, 99%) and divinyl benzene (DVB, 50%) as the crosslinking agent were obtained from the Sigma-Aldrich Co. (New York, USA). Benzoyl peroxide (BPO, 75%) (used as an initiator) and poly(vinyl alcohol) (PVA) (used as a stabilizer) were purchased from Lancaster (Morecambe, England) and Junsei, respectively. 1-(2-Pyridylazo)-2-naphtol (PAN), acetonitrile (used as a

diluent), and ethylene diamine tetracetic acid (EDTA) (used as an indicator and as a titrant) were purchased from the Sigma-Aldrich Co. (New York, USA) and Samchun Co. (Seoul, Korea), respectively.

2.2. Synthesis of the Bifunctional Poly(VPA-*co*-GMA-*co*-DVB) Cation-Exchangers

The highly selective bifunctional poly(VPA-*co*-GMA-*co*-DVB) cation exchangers were synthesized by suspension polymerization [10,11-13]. **Table 1** and **Figure 1** show the synthesis conditions, the polymerization scheme and the functionalization of the poly(VPA-*co*-GMA-*co*-DVB) cation exchangers with iminodiacetic acid, respectively. The polymerization was conducted in a 1000 mL four-neck round-bottom flask equipped with a mechanical stirrer (IKA® RW20 digital, IKA company, Osaka, Japan), a condenser, a nitrogen inlet, a thermometer and a dropping funnel. VPA, GMA and DVB were dissolved in acetonitrile (ACN) and PVA at 70˚C. The solution was placed under continuous, strong agitation until all of the monomers and 2,2'-Azobis isobutyro nitile (AIBN), which was used as an initiator, were completely dissolved. The polymerization was performed in airtight equipment at 70˚C and maintained with stirring (400 rpm) for 24 hours. The bifunctional poly(VPA-*co*-GMA-*co*-DVB) resins were separated by vacuum suction and washed using distilled water until a pH of 7 was achieved. The poly(VPA-*co*-GMA-*co*-DVB) resins were dried in a vacuum oven for 24 hours at 50˚C. The yield of the copolymer resins was determined using Equation (1):

$$\text{Synthetic yield } (\%) = W_d / W_m \times 100 \qquad (1)$$

where W_d is the weight of clean and dry polymer beads (g) and W_m is the initial weight of the monomer (g).

2.3. Functionalization Reaction of Poly(VPA-*co*-GMA-*co*-DVB) Resins by Iminodiacetic Acid

The bifunctionalized poly(VPA-*co*-GMA-DVB) cation

Table 1. Synthesis conditions of poly(VPA-*co*-GMA-*co*-DVB) cation exchange resins.

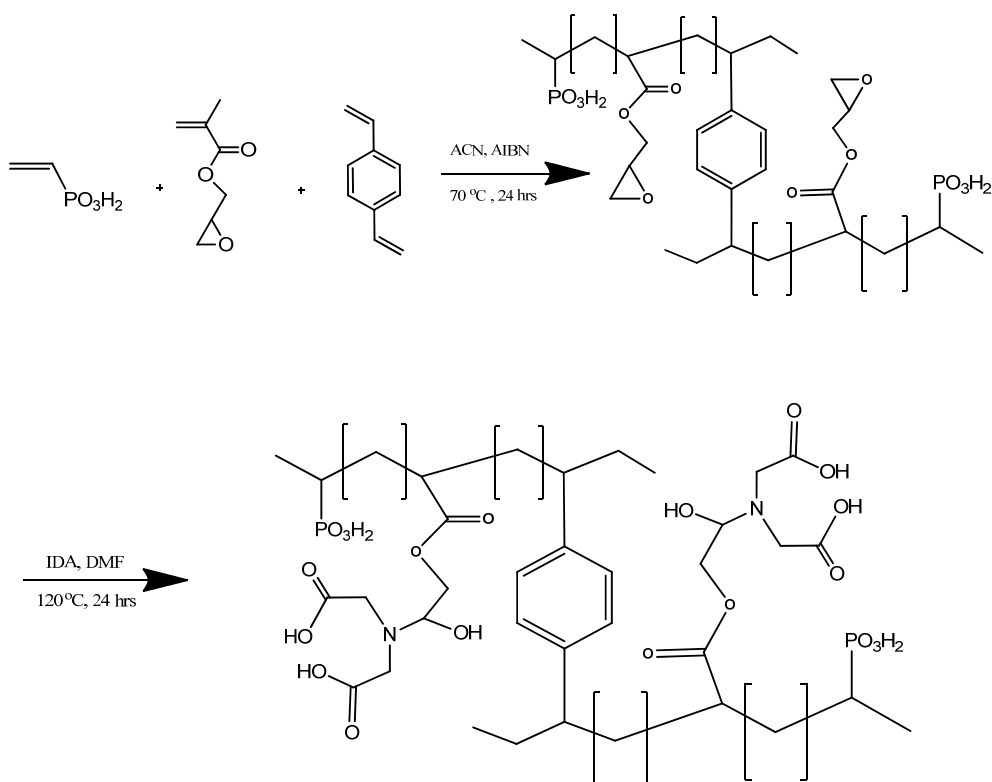| Batch NO.	Monomer			AIBN (Wt%)	Medium ACN (g)	Temp. (˚C)	Duration (h)	Conversion (%)
	GMA	VPA	DVB					
PVGD-1	100	0	0	4	23	70	24	83
PVGD-2	70	10	20	4	23	70	24	95
PVGD-3	60	20	20	4	23	70	24	89
PVGD-4	50	30	20	4	23	70	24	85
PVGD-5	40	40	20	4	23	70	24	70
PVGD-6	30	50	20	4	23	70	24	62

Figure 1. A schematic mechanism of PVGD and IPVGD cation-exchange resin.

exchangers were functionalized using iminodiacetic acid. **Table 2** shows the functionalization conditions. The reaction for functionalizing the poly(VPA-*co*-GMA-*co*-DVB) cation exchangers was conducted in a 500 mL four-neck round-bottom flask equipped with a mechanical stirrer (IKA® RW20 digital, IKA company, Osaka, Japan), a condenser, a nitrogen inlet, a thermometer and a dropping funnel. The poly(VPA-*co*-GMA-*co*-DVB) copolymer was placed in the reactor with 300 mL of DMF. The functionalization was performed at 120°C for 24 hours with stirring (400 rpm). After introducing the IDA groups in the GMA of the copolymer, the remaining unreacted epoxide groups were hydrolyzed with a dilute HCl solution for 2 hr at 80°C. Subsequently, the poly (VPA-*co*-GMA-*co*-DVB) cation exchangers with IDA groups were washed with methanol and then dried at 50°C in a vacuum oven.

2.4. Characterization of Poly(Vinyl Phosphonic Acid-*co*-metacrylic Acid)

The structures of the poly(VPA-*co*-GMA-*co*-DVB) resins and the bifunctional poly(VPA-*co*-GMA-*co*-DVB) cation exchangers were characterized using a FT-IR spectrometer (IR Prestige-21, Shimadzu, Kyoto, Japan). The KBr pellets, which contained 1 mg of the sample and 150 mg of KBr, were prepared on a press using a 60 - 70 kN of compression force for 10 minutes under vacuum.

The FT-IR spectra were obtained over a wavenumber range of 4000 - 600 cm^{-1}, the resolution was 4 cm^{-1}, and 20 scans were recorded.

The morphologies of the poly(VPA-*co*-GMA-*co*-DVB) cation exchangers were analyzed using a scanning electron microscope (SEM), and the elemental analyses of these exchangers were conducted using energy dispersive X-ray spectroscopy (EDS, JSM-7000F, JEOL, Akishima, Japan). Incident electron-beam energies from 0.5 to 30 keV were used. In all cases, the beam was at a normal incidence to the sample surface, and the measurement time was 100 s. All of the surfaces of the samples were covered with osmium using the ion sputtering method.

The acidic resistance of the PVGD and IPVGD cation exchange resins was investigated using the weight measurement method. One gram of resin and a 5% HCl standard solution (30 ml) were placed in a 50 ml Erlenmeyer flask. The flask was placed in a shaking water bath at 50°C. The resin was removed from the flask after 60 minutes, washed with distilled water and dried in a heating oven at 50°C. The durability was calculated using Equation (2):

$$\text{Durability } (\%) = (W_w - W_d)/W_d \times 100\% \qquad (2)$$

where W_w and W_d are the weights of the sample before and after treatment with acid, respectively.

The crush strength of the PVGD and IPVGD cation exchange resins before and after acid treatment were

Table 2. Functionalization conditions of poly(VPA-*co*-GMA-*co*-DVB).

Batch No.	PVGD (g)	IDA (g)	DMF (g)	Temp. (°C)	Time (hr)	Conversion (%)
IPVGD-1	20	20	300	120	24	80
IPVGD-2	20	20	300	120	24	91
IPVGD-3	20	20	300	120	24	88
IPVGD-4	20	20	300	120	24	83
IPVGD-5	20	20	300	120	24	68
IPVGD-6	20	20	300	120	24	60

tested with a universal testing machine (UTM). The specimens were prepared according to the ASTM standard. All specimens were measured 5 times.

2.5. Water Uptake and Cation Exchange Capacity

A 1 g, dried sample was immersed in DI water for 24 hr. The sample was removed from the DI water and wiped with absorbent paper to remove excess water adhered to the surface. The sample was then weighed on a balance. The water uptake was calculated using Equation (3) [14,15]:

$$\text{Water uptake } (\%) = (W_w - W_d)/W_d \times 100 \qquad (3)$$

where W_w and W_d are the weights of the sample in wet and dry conditions, respectively.

Titration was used to determine the ion-exchange capacity (IEC) of the cation exchange resins. The sample was equilibrated in 100 mL of a 0.1 N NaOH solution at room temperature for 24 hr before it was removed, and then 20 mL of the NaOH solution was titrated with a 0.1 mol/L HCl solution, which contained a drop of phenolphthalein solution (0.1% in ethanol) as a pH indicator. The experimental IEC was calculated according to Equation (4):

$$\text{IEC } (meq/g) = ((V_{\text{NaOH}} \times C_{\text{NaOH}}) - (5 \times V_{\text{HCl}} \times C_{\text{HCl}}))/W_d \qquad (4)$$

where V_{NaOH} and V_{HCl} are the volume of the NaOH solution and the consumed volume of the HCl solution, respectively. C_{NaOH} and C_{HCl} are the concentrations of NaOH and HCl, respectively.

2.6. Indium Adsorption Property

Experiments examining the adsorption of indium from pure and artificial ITO solutions (see **Table 3**) were conducted under ambient conditions using the batch technique. The experiments examining the adsorption onto the bifunctional poly(VPA-*co*-GMA-*co*-DVB) cation exchange resins were performed at pH 4. The pH values

Table 3. Chemical composition of artificial ITO waste water.

Salt	Mw	Metalic Mass	wt%	g/L
NaCl (35% ~ 37%)				
In-In(Cl)3*4H$_2$O	293.24	114.82	0.391	0.2472
Sn-Tin(II) chloride dihydrate	225.60	118.74	0.526	0.0168
Si-Na$_2$O$_3$Si	122.06	28.08	0.230	0.0034
Al-AlCl$_3$*6(H$_2$O)	241.43	26.98	0.111	0.0017
Ca-CaCl$_2$*2H$_2$O	128.99	40.07	0.310	0.0004
Fe-Ferric pyrophosphate	745.21	55.84	0.074	0.0020

were adjusted with a negligible amount of a 0.01 or 0.1 M HCl or NaOH standard solution. Twenty-five milligrams of the bifunctional poly(VPA-*co*-GMA-*co*-DVB) cation exchange resins were immersed in a 50-mL indium solution, and the cation exchange resins were mixed with an indium solution in a shaker, which was operated at 200 rpm for 24 hr to reach equilibrium.

The indium adsorption property was determined using the EDTA titration method. A certain amount of sample was immersed in a 100 mg/L indium solution, and then 40 mL was taken from the indium solution. 1-(2-Pyridylazo)-2-naphtol (PAN) was used as an indicator. The amount of adsorbed indium was calculated using Equation (5):

$$\text{Amount of adsorbed indium } (mmol/g)$$
$$= (C_{In}V_{in} - 2.5 \times C_{ETDA}V_{EDTA})/W_{resin} \qquad (5)$$

where C_{in} and V_{in} are the molar concentration and the volume of the initial indium solution, respectively. C_{EDTA} and V_{ETDA} are the molar concentration and the consumed volume of the EDTA solution, respectively.

2.7. Durability Test

The bifunctional poly(VPA-co-GMA-co-DVB) microbeads that had adsorbed indium were dipped into a solution of 0.1 mol/L HCl with stirring for 4 hr at 25°C to

desorb indium (III) ions. The solution was then filtered and washed with water. The obtained bifunctional poly(VPA-*co*-GMA-*co*-DVB) microbeads were used in the adsorption experiment. This entire process was repeated for 10 cycles to ascertain the reusability of the bifunctional poly(VPA-*co*-GMA-*co*-DVB) microbeads.

3. Results and Discussion

3.1. Preparation of PVGD and IPVGD Cation-Exchange Resins

Figure 2 shows the conversions of the poly(VPA-*co*-GMA-*co*-DVB) resins and the bifunctional poly(VPA-*co*-GMA-*co*-DVB) cation exchanger. The conversions were calculated from Equation (1), where the initial weights of the monomers revealed the weights before the synthesis of the poly(VPA-*co*-GMA-*co*-DVB) resins in the cases of both synthesis and functionalization. The conversion was increased slightly to increase the GMA molar ratio, and the maximum conversion was 93%. The use of divinyl benzene (DVB) as a crosslinking agent did not affect the conversion. However, the conversions of the bifunctional poly(VPA-*co*-GMA-*co*-DVB) cation exchanger ranged between 85% and 93%, and the values increased with increasing GMA molar ratio.

3.2. Structure Analysis

Figure 3 shows the FT-IR spectra for confirming the structure and functionalization of poly(vinyl phosphonic acid-*co*-glycidyl methacrylate-co-divinyl benzene) (PVGD) and poly(vinyl phosphonic acid-*co*-glycidyl methacrylate-co-divinyl benzene) containing iminodiacetic acid group (IPVGD) cation exchange resins. As shown in **Figure 3(a)** (PVGD spectrum), the strong broad band at approximately 3500 cm^{-1} was attributed to OH vibrations. The bands resulting from methylene C-H stretching vibrations were observed at approximately 2941 cm^{-1}. The strong band at 1194 cm^{-1} was ascribed to the stretching vibrations of P=O, and the absorption band at 965 cm^{-1} was ascribed to the P-OH stretching band. In addition, a strong band at 1720 cm^{-1} resulted from C=O stretching vibrations in GMA, and the other band at 450 - 1650 cm^{-1} was due to stretching vibrations in the vinyl groups of DVB. These results confirmed which PVGD cation exchange resins were synthesized. **Figure 3(b)** shows the FT IR spectrum of poly(vinyl phosphonic acid-*co*-glycidyl methacrylate-co-divinyl benzene) containing iminodiacetic acid group (IPVGD) cation exchange resins. The strong band at 1660 cm^{-1} was attributed to COOH vibrations, and the intensity of the broad band at approximately 3450 cm^{-1}, which was attributed to OH, was increased. This result confirmed which IPVGD cation exchange resin was synthesized [16].
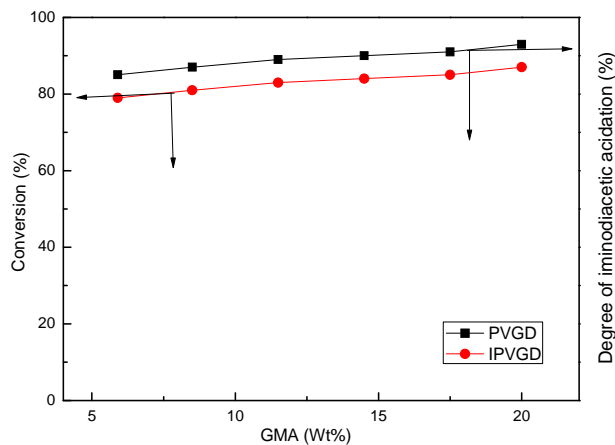

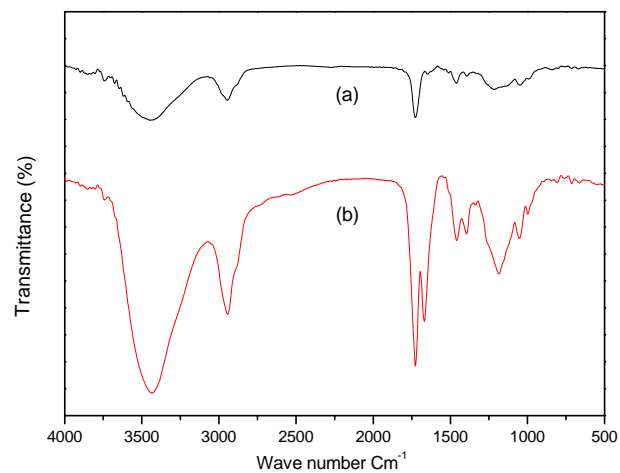**Figure 2. The effect of the GMA content on the conversion.**

Figure 3. FT-IR spectra of PVGD and IPVGD cation-exchange resin: (a) PVGD and (b) IPVGD.

3.3. SEM-EDS of PVGD and IPVGD Cation-Exchange Resins

Figure 4 and **Table 4** show the morphological evaluations and the elemental compositions of the PVGD and bifunctional IPVGD cation exchange resins determined using SEM-EDS analyses. The surfaces of the resins were smoothly spheres, and their average particle sizes were approximately 50 μm. **Figure 4** shows SEM photographs of the resins. The morphologies of the resins before and after functionalization were not observed to be different in PVGD and IPVGD.

Table 4 shows the proportions of carbon, oxygen and phosphorous in the PVGD and IPVGD resins. The phosphorus oxygen contents were determined to be 1.00%, 1.96%, 2.68% and 3.76%, respectively, in the PVGD resins. Their contents were increased by increasing the VPA monomer ratio. Meanwhile, the oxygen compositions for IPVGD resins were higher than that of PVGD. Their values were 1.00%, 1.96%, 2.68% and 3.76%, respectively. These results confirmed which
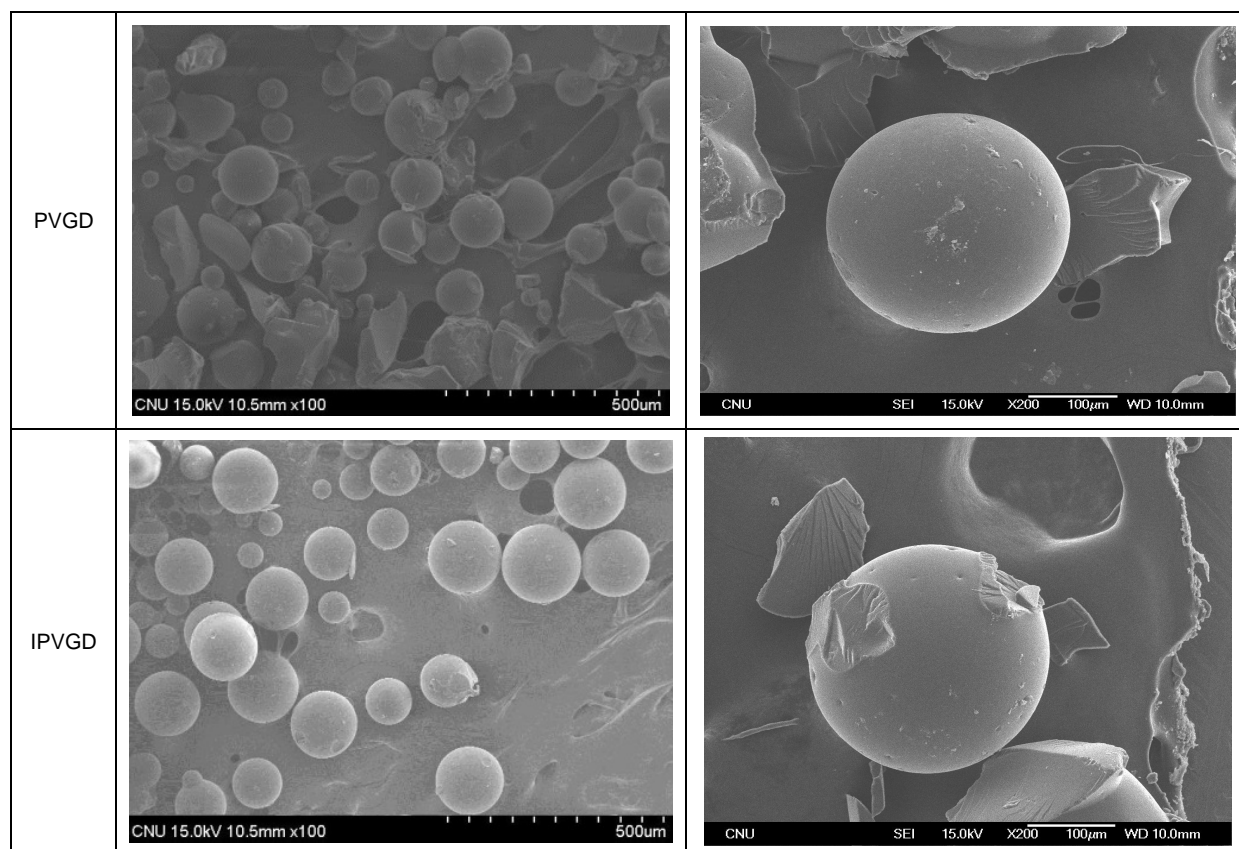
Figure 4. SEM photographs of PVGD and IPVGD resins.

Table 4. Chemical composition of PVGD and IPVGD resins by EDS analysis.

Batch No	Carbon(wt%)	Oxygen(wt%)	Phosphorus(wt%)
PVGD-1	54.84	35.37	9.79
PVGD-2	70.11	25.56	4.17
PVGD-3	66.79	27.35	5.71
PVGD-4	64.26	26.96	8.77
PVGD-5	63.08	28.74	7.04
IPVGD-1	73.20	23.39	3.41
IPVGD-2	68.52	25.30	6.18
IPVGD-3	66.32	25.61	8.07
IPVGD-4	63.03	26.97	10.00
IPVGD-5	61.20	29.40	9.40

bifunctional IPVGD cation exchange resins were synthesized using iminodiacetic acid.

3.4. Water Uptake and Ion-Exchange Capacity of PVGD and IPVGD Cation Exchange Resins

Figure 5 shows the effect of divinyl benzene on the water uptake of the PVGD and IPVGD resins. The water uptake was decreased with increasing DVB contents. The water uptakes of the IPVGD resins were higher than those of PVGD because the hydrophilicity of the resins increased due to the carboxyl group. The crosslinking ratios were also determined to affect the water uptake of the hydrophilic polymers. The water uptake was also dependent on the amount of crosslinking agent. The water uptake values decreased to a minimum of 75% as a result of the increased crosslinking density of the resins.

The IEC provides an indication of the acid group content in the PVGD and IPVGD resins. The experimental IEC values are given in **Figure 6**. This result confirmed that the IEC values decreased. The IEC values of the PVGD and IPVGD resins were 2.5 - 5.6 meq/g and 2.7 - 6.4 meq/g, respectively. In addition, the values for the IPVGD resins were higher than those of the PVGD resins because of the increase of the hydrophilicity due to the introduction of the COOH groups. This result led to the conclusion that the IPVG resins were acceptable adsorbents for indium from ITO and the dilute solutions.

3.5. Indium Adsorption Properties

Adsorption isotherm experiments to examine the adsorption of indium on the cation-exchange resin were performed at pH 4. The cation-exchange resin was placed in
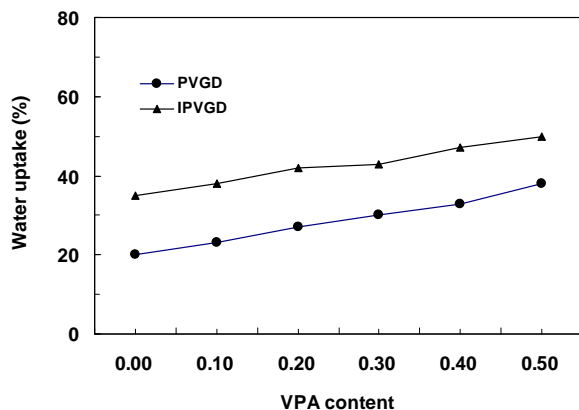
OJPChem

Figure 5. The effect of DVB mole ratio on the water uptake.

Figure 7. Adsorption isotherms of In^{3+} onto the cation-exchange resin by (a) Freundlich and (b) Langmuir model.
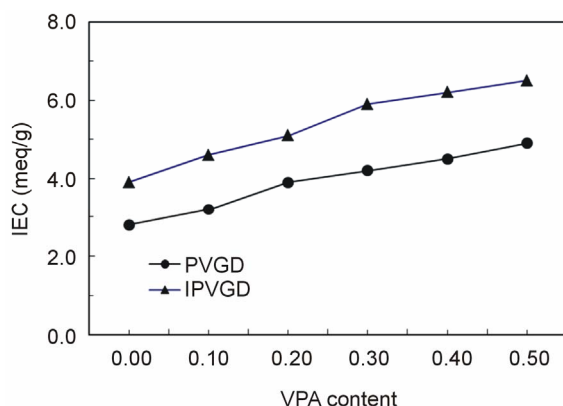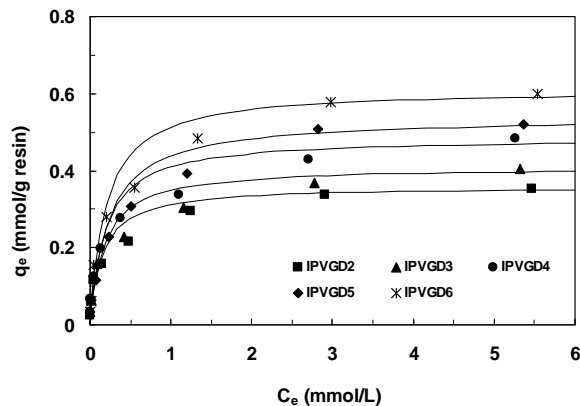

Figure 6. The effect of DVB mole ratio on the ion-exchange capacity.

contact with the solution in a shaker operating at 200 rpm at 25°C for 4 hr to reach equilibrium. The Langmuir and Freundlich equations were applied to the adsorption equilibria for the micro-bead [17-20]:

$$C_e/q_e = 1/(K_L q_m) + C_e/q_m \qquad (5)$$

$$q_e = K_F C_e^{1/n} \qquad (6)$$

where C_e is the equilibrium concentration (mmol/L), q_e is the adsorption capacity at equilibrium (mmol/g resin) and q_m is the maximum amount of solute exchanged per gram of micro-beads (mmol/g resin). K_L and K_F are the Langmuir constant and the Freundlich constant related to the adsorption capacity, respectively, and n is a constant to be determined.

Figure 7 shows the experimental adsorption isotherms of In^{3+} on the cation-exchange resin. **Figures 8(a)** and **(b)** are the linear plots of the Freundlich and Langmuir models obtained from the experimental data in **Figure 7**. All constants derived from **Figure 7** are listed in **Table 3**. Finally, the Langmuir and Freundlich models calculated from the data in **Table 5** are also illustrated in **Figure 7**. The Langmuir constants, such as K_L and q_m, were obtained using the linear plot of C_e/q_e vs. C_e from Equa-
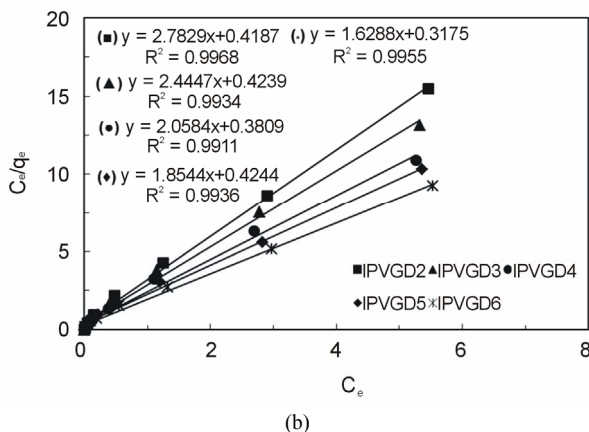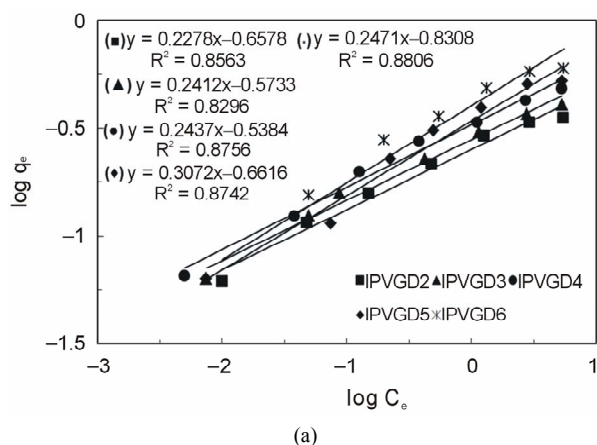

(a)

(b)

Figure 8. Isotherm analyses of the adsorption of In^{3+} onto the cation-exchange resin by (a) Freundlich and (b) Langmuir model.

tion (5), and the Freundlich constants, such as K_F and n, were determined with the plot of $\log q_e$ vs. $\log C_e$ from Equation (6).

As shown in **Figure 7**, the experimental data corresponded better to the Langmuir model. A basic assumption of the Langmuir model is that the adsorption occurs at specific, homogeneous sites in the adsorbent; thus, it is

Table 5. Isotherm constants for the adsorption of In³⁺ onto the cation-exchange resin.

Sample code	Langmuir model			Freundlich model		
	K_L	q_m	R^2	K_F	n	R^2
IPVGD2	6.647	0.359	0.997	0.518	4.390	0.856
IPVGD3	5.767	0.409	0.993	0.564	4.146	0.829
IPVGD4	5.404	0.486	0.991	0.584	4.103	0.876
IPVGD5	4.369	0.539	0.994	0.516	3.255	0.874
IPVGD6	5.130	0.614	0.996	0.436	4.047	0.881

confined to a monolayer of adsorption, whereas the Freundlich model considers equilibrium on a heterogeneous surface, where the adsorption energy is not homogeneous for all adsorption sites. Thus, the Freundlich model can be applied to multi-layer adsorption. Therefore, the adsorption behavior of In³⁺ on the IPVGD cation-exchange resin is considered to be the adsorption of a monolayer.

The maximum value of q_m, the maximum amount of solute exchanged per gram of poly(GMA-*co*-PEGDA) microbeads, was attained at a 90% molar ratio of GMA, and the value was 0.614 mmol/g resin.

3.6. Acidic Resistance

The indium adsorbents endured in the strong acid solution because the pH of the ITO etching solution was low. Thus, this experiment measured the acid resistance of the PVGD and IPVGD resins. **Figure 9** shows the result for the acidic resistance for the PVGD and IPVGD resins. The weight losses of the PVGD and IPVGD resins were minimal. According to this result, the PVGD and IPVGD resins were very excellent in the low pH solution. In general, the acidic resistance was influenced by the degree of crosslinking of the resins. The degree of crosslinking of the PVGD and IPVGD resins increased with increasing DVB content in the resins. When the degree of crosslinking was increased, the skeletal structure of the resins increased the rigidity. Thus, the mechanical strength was higher than that before crosslinking.

3.7. Durability

The durability was also investigated. The maximum sorption capacity changes of indium versus the number of reuses are provided in **Figure 10** for up to 10 reuses. Each of the maximum sorption capacities according to the number of reuse times was obtained from Equation (6). It is observed that the maximum sorption capacity of indium onto PVGD and IPVGD decreased only slightly with an increasing number of reuse times, which indicates that the prepared microbeads have a good reusability.
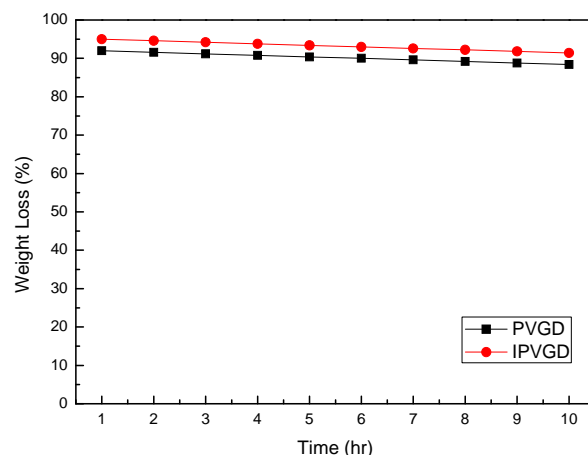
Figure 9. Acidic resistance of PVGD and IPVGD resins against 5% HCl.
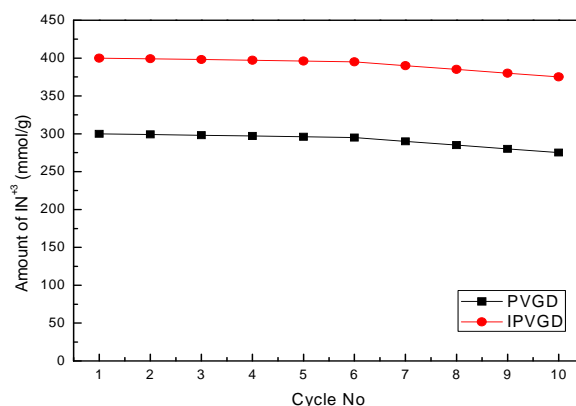
Figure 10. The effect of cycleization number on the durability onto PVGD and IPVGD resins for 30 minutes.

4. Conclusion

PVGD and IPVGD, which have indium ion selectivities, were synthesized by suspension polymerization and their indium adsorption properties were investigated. The conversions of the bifunctional poly(VPA-*co*-GMA-*co*-DVB) cation exchanger ranged between 85% and 93%, and the values increased with increasing GMA molar ratio. The synthesized PVGD and IPVGD resins were characterized using Fourier transform infrared (FTIR) spectroscopy, scanning electron microscopy (SEM), and energy-dispersive X-ray spectroscopy (EDS). According to the FTIR result, it was confirmed that the IPVGD cation exchange resin was synthesized. The surfaces of the resins were wrinkled spheres, and their average particle sizes were approximately 50 μm. However, the morphology of resins before and after functionalization did not show a difference between PVGD from IPVGD. The contents were increased by increasing the VPA monomer ratio. The water uptakes of IPVGD resins were higher than those of PVGD because the hydrophilicity of the resins increased due to the carboxyl group. The IEC val-

ues increased as the DVB concentration decreased, which was accompanied by a consequential increase in the GMA concentration. When the degree of crosslinking was increased, the skeletal structure of the resins increased in rigidity.

5. Acknowledgements

REFERENCES

[1] S. Virolainene, D. Ibana and E. Paatero, "Recovery of Indium from Indium Tin Oxide by Solvent Extraction," *Hydrometallurgy*, Vol. 107, No. 1, 2011, pp. 56-61. http://dx.doi.org/10.1016/j.hydromet.2011.01.005

[2] T. Kato, S. Igarashi, Y. Ishiwatari,Y. Ishiwatari, M. Furukawa and H. Yamaguchi, "Separation and Concentration of Indium from a Liquid Crystal Display via Homogeneous Liquid-Liquid Extraction," *Hydrometallurgy*, Vol. 137, 2013, pp. 148-155. http://dx.doi.org/10.1016/j.hydromet.2013.06.004

[3] H. Hasegawa, I. M. M. Rahman, Y. Egawa and H. Sawai, "Chelant-Induced Reclamation of Indium from the Spent Liquid Crystal Display Panels with the Aid of Microwave Irradiation," *Journal of Hazardous Materials*, Vol. 254-255, 2013, pp. 10-17.

[4] J. Ruan, Y. Guo and Q. Qiao, "Recovery of Indium from Scrap TFT-LCDs by Solvent Extaction," *Procedia Environmental Sciences*, Vol. 16, 2012, pp. 545-551.

[5] H. Minamisawa, K. Murashima, M. Minamisawa, N. Arai and T. Okutani, "Determination of Indium by Graphite Furnace Atomic Absorption Spectrometry after Coprecipitation with Chitosan," *Anaytical Sciences*, Vol. 19, No. 3, 2003, pp. 401-404. http://dx.doi.org/10.2116/analsci.19.401

[6] M. Tuzen and M. Soylak, "A Solid Phase Extraction Procedure for Indium Prior to Its Graphite Furnace Atomic Absorption Spectrometric Determination," *Journal of Hazardous Materials*, Vol. 129, No. 1, 2006, pp. 179-185. http://dx.doi.org/10.1016/j.jhazmat.2005.08.031

[7] I. M. M. Kenawy, M. A. H. Hafez and S. A. Elwaness, "Preconcentration and Separation by Electrodeposition of Indium from Its Different Solution Complexes," *Bulletin de la Société Chimique de France*, Vol. 5, 1991, pp. 677-683.

[8] H. Liu, C. Wu, Y. Lin and C. Chiang, "Recovery of Indium from Etching Wastewater Using Supercritical Carbon Dioxide Extraction," *Journal of Hazardous Materials*, Vol. 172, No. 2-3, 2009, pp. 744-748. http://dx.doi.org/10.1016/j.jhazmat.2009.07.098

[9] W. Chou and Y. Huang, "Electrochemical Removal of Indium Ions from Aqueous Solution Using Iron Electrodes," Vol. 172, No. 1, 2009, pp. 46-53.

[10] O. Acar and A. R. Türker, "Determination of Bismuth, Indium and Lead in Spiked Sea Water by Electrothermal Atomic Absorption Spectrometry Using Tungsten Containing Chemical Modifiers," *Spectrochimica Acta Part B*, Vol. 55, No. 10, 2000, pp. 1635-1641. http://dx.doi.org/10.1016/S0584-8547(00)00258-5

[11] N. Kabay, S. Sarp, M. Yuksel, Ö. Arar and M. Bryjak, "Removal of Boron from Seawater by Selective Ion Exchange Resins," *Reactive & Functional Polymers*, Vol. 67, 2007, pp. 1643-1650. http://dx.doi.org/10.1016/j.reactfunctpolym.2007.07.033

[12] M. Tuzen and M. Soylak, "A Solid Phase Extraction Procedure for Indium Prior to Its Graphite Furnace Atomic Absorption Spectrometric Determination," *Journal of Hazardous Materials*, Vol. 129, No. 1, 2006, pp. 179-185. http://dx.doi.org/10.1016/j.jhazmat.2005.08.031

[13] F. M. B. Coutinho, D. L. Carvalho, M. L. L. T. Aponte and C. C. R. Barbosa, "Pellicular Ion Exchange Resins Based on Divinylbenzene and 2-Vinylpyridine," *Polymer*, Vol. 42, No. 1, 2001, pp. 43-48. http://dx.doi.org/10.1016/S0032-3861(00)00343-8

[14] K. S. Shin, E. M. Choi and T. S. Hwang, "Preparation and Characterization of Ion-Exchange Membrane Using Sty/HEA/LMA Terpolymer via Post-Sulfonation," *Desalination*, Vol. 263, No. 1, 2010, pp. 151-158. http://dx.doi.org/10.1016/j.desal.2010.06.052

[15] Z. Wang, H. Ni, M. Zhang, C. Zhao and H. Na, "Preparation and Characterization of Sulfonated Poly(arylene ether ketone sulfone)s for Ion Exchange Membranes," *Desalination*, Vol. 242, No. 1-3, 2009, pp. 236-244 http://dx.doi.org/10.1016/j.desal.2008.05.003

[16] R. M. Silverstein, F. X. Webster and D. J. Kiemle, "Spectrometric Identification of Organic Compounds," John Wiley & Sons, Inc., New York, 2005.

[17] W. Lin, L. T. Biegler and A. M. Jacobson, "Modeling and Optimization of a Seeded Suspension Polymerization Process," *Chemical Engineering Science*, Vol. 65, No. 15, 2010, pp. 4350-4362. http://dx.doi.org/10.1016/j.ces.2010.03.052

[18] K. Jia, B. Pan, Q. Zhang, W. Zhang, P. Jiang, C. Hong, B. Pan and Q. Zhang, "Adsorption of Pb^{2+}, Zn^{2+}, and Cd^{2+} from Waters by Amorphous Titanium Phosphate," *Journal of Colloid and Interface Science*, Vol. 318, No. 2, 2008, pp. 160-166. http://dx.doi.org/10.1016/j.jcis.2007.10.043

[19] C. A. P. Almeida, A. dos Santos, S. Jaerger, N. A. Debacher and N. P. Hankins, "Mineral Waste from Coal Mining for Removal of Astrazon Red Dye from Aqueous Solutions," *Desalination*, Vol. 264, No. 3, 2010, pp. 181-187. http://dx.doi.org/10.1016/j.desal.2010.09.023

[20] B. Mandal and N. Ghosh, "Extraction Chromatographic Method of Preconcentration and Separation of Lead (II) with High Molecular Mass Liquid Cation Exchanger," *Desalination*, Vol. 250, No. 2, 2010, pp. 506-514. http://dx.doi.org/10.1016/j.desal.2009.06.050